

Cell Reports, Volume 42

## Supplemental information

**Dynamic genetic adaptation**

**of *Bacteroides thetaiotaomicron***

**during murine gut colonization**

**Megan S. Kennedy, Manjing Zhang, Orlando DeLeon, Jacie Bissell, Florian Trigodet, Karen Lolans, Sara Temelkova, Katherine T. Carroll, Aretha Fiebig, Adam Deutschbauer, Ashley M. Sidebottom, Joash Lake, Chris Henry, Phoebe A. Rice, Joy Bergelson, and Eugene B. Chang**

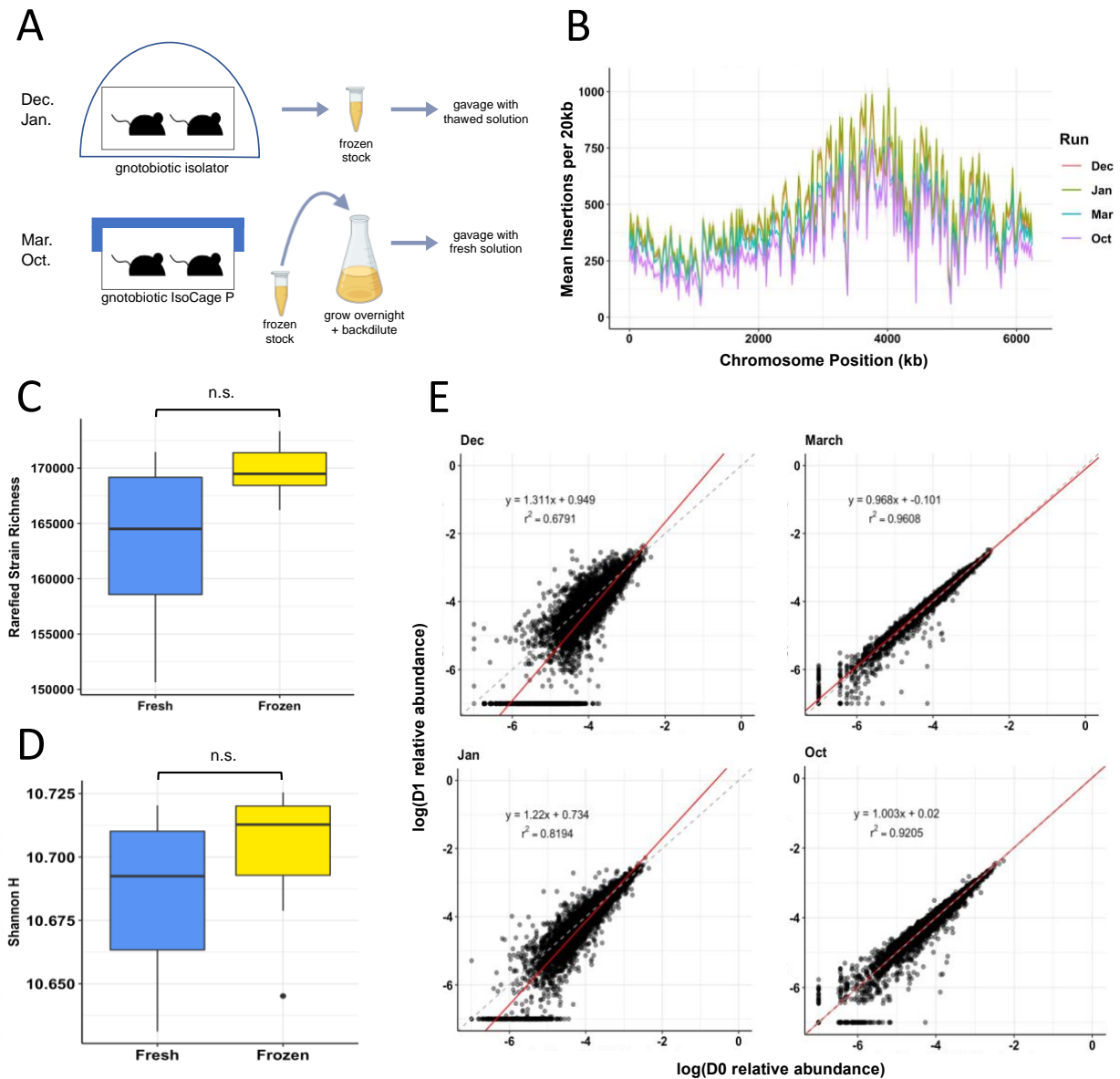


**Fig. S1: Comparison of functional genetics experimental protocols and outcomes.** A) Schematic representation of protocol differences across experimental cohorts. In Dec. and Jan. cohorts, mice were housed in cages of 2-3 animals within gnotobiotic isolators and gavaged with thawed stocks; in Mar. and Oct. cohorts, mice were housed in gnotobiotic cages of 2-3 animals on an IsoCage P Bioexclusion rack system and gavaged with stocks that had been grown overnight in fresh media. B) Mean number of unique mutant strains with RB-Tn insertions identified per 20kb region in inoculum samples from each experimental cohort. C) Rarefied strain richness is not significantly different across fresh and frozen inocula (two-sided Wilcoxon rank sum test,  $p = 0.09$ ,  $n = 8-13$  per group). Samples were rarefied due to uneven sequencing depth across experimental cohorts. D) Shannon diversity is not significantly different across fresh and frozen inocula (two-sided Wilcoxon rank sum test,  $p = 0.1774$ ). E) Comparison of inoculum (D0) versus D1 relative abundance of each RB-Tn gene mutant. Dashed line represents 1:1, red line and equation represent linear regression best-fit line. Cohorts with frozen inoculum (Dec, Jan) experienced greater loss of mutants with low D0 relative abundance ( $< 0.0001$ ) compared to cohorts with fresh inoculum (Mar, Oct).

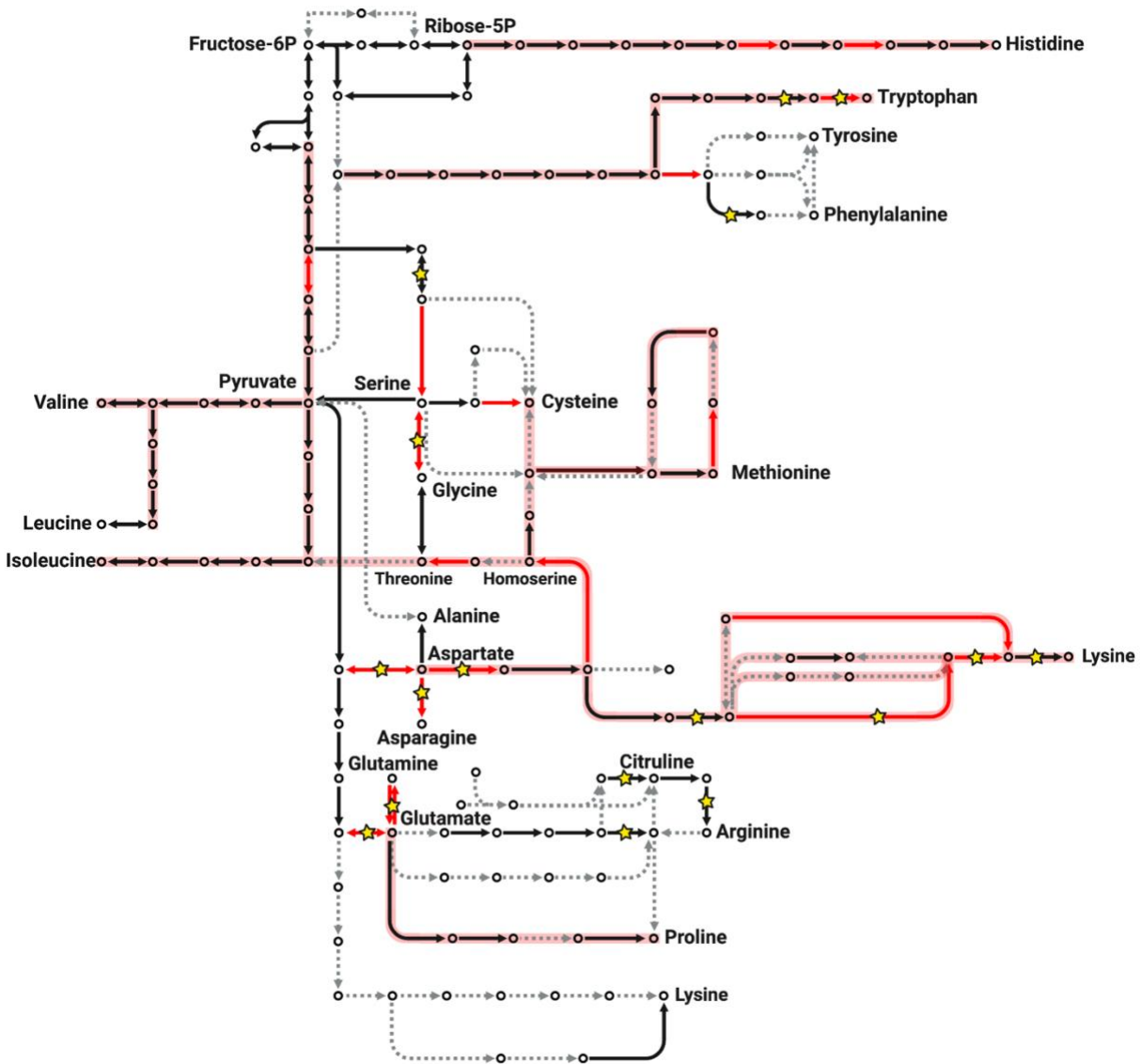


**Fig. S2: Pathway map of reactions related to amino acid biosynthesis.** Red arrows represent specific genes whose transcript is significantly enriched on D0.5/1 relative to D2/4 ( $\log\text{FDR} < -3$ ,  $|\log_2\text{FC}| > 2$ , and base mean  $> 50$  RPM), and red highlight represents pathways that were overall enriched on D0.5/1 relative to D2/4 ( $p_{\text{adj}} < 0.05$ ). No genes or pathways on this map were relatively more expressed at D2/D4 than D0.5/D1. Genes whose transcript level did not differ significantly between D0.5/1 and D2/4 are colored in black. Grey dashed arrows represent reactions for which the associated gene is unknown in the *Bt* genome. Gold stars represent gene disruptions that were depleted in the RB-Tn assay, as in Fig. 2C. See also Table S6.

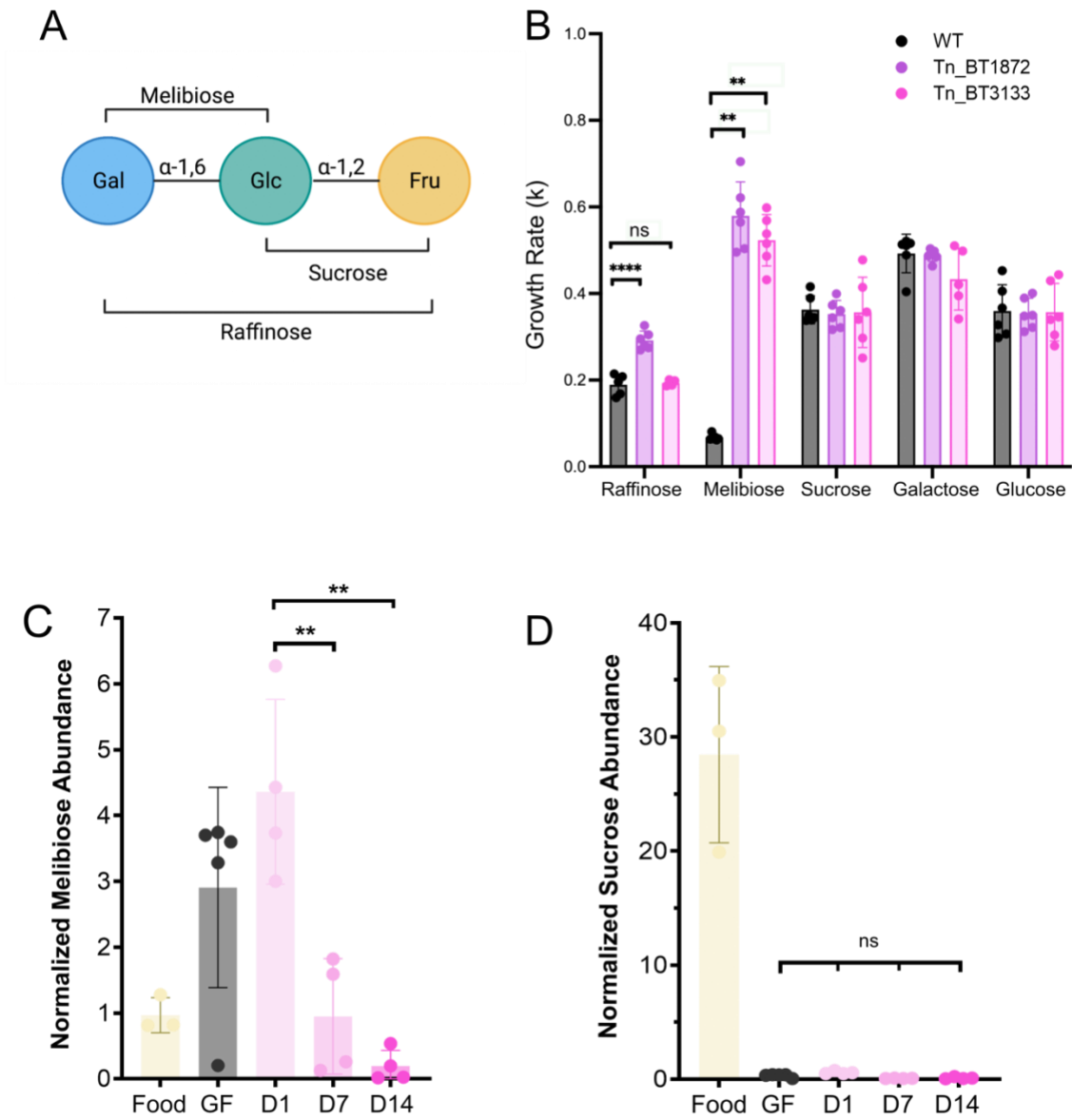


**Fig. S3: *Bt* adapts to the GF gut specifically by increasing efficiency of metabolizing  $\alpha$ -1,6 bonded sugars.** A) Structure of the trisaccharide raffinose. B) The log phase doubling times of Tn\_BT3133 and Tn\_BT1872 were measured in Varel-Bryant medium with 20 mM raffinose, melibiose, sucrose, galactose, or glucose as the sole carbon substrate. Abundance of C) melibiose or D) sucrose in the standard chow fed to GF mice, within GF ceca before colonization, or 1, 7, or 14 days post-colonization.

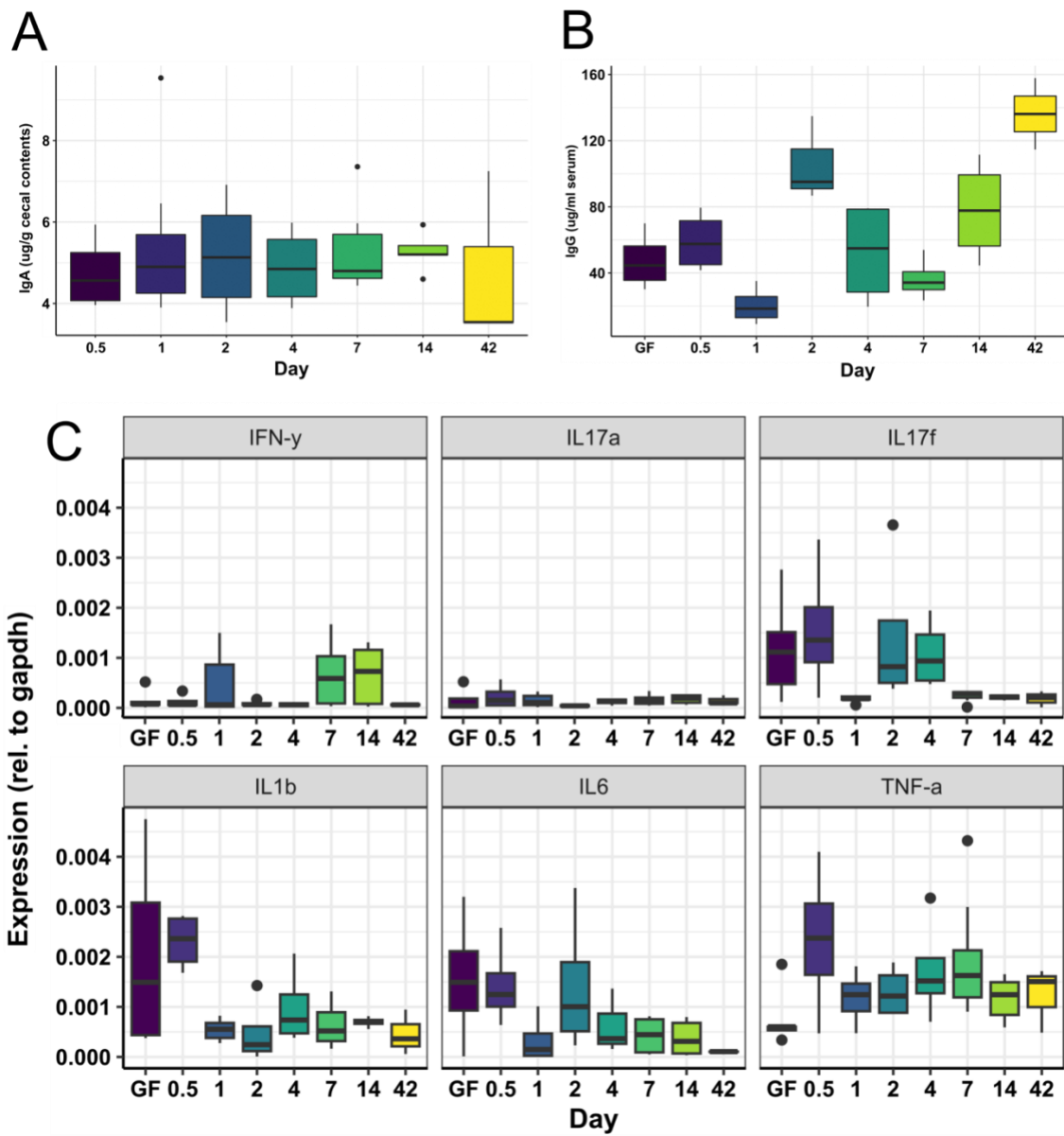


**Fig. S4: *Bt* does not elicit a strong temporal host response.** A) Cecal IgA and B) serum IgG levels from mice sacrificed at different timepoints after colonization (n=3-4/timepoint). C) Cytokine expression relative to gapdh in colonic mucosal scrapings at different timepoints after colonization (n=4-6/timepoint).

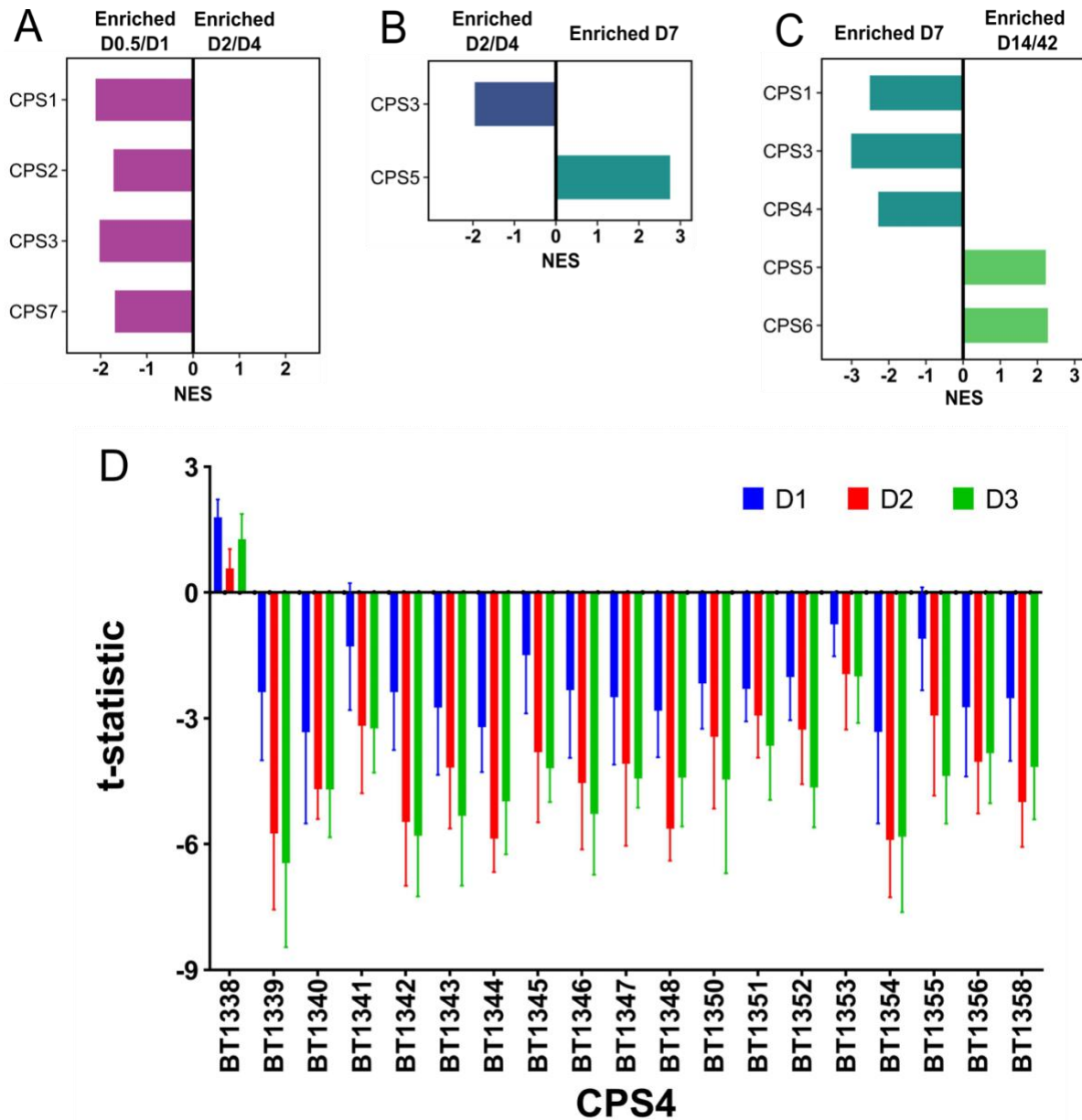


**Fig. S5: Capsular polysaccharide biosynthesis operons are significantly associated with different stages of colonization.** (A – D) Gene set enrichment analysis (GSEA) using transcriptomics data for capsular polysaccharide biosynthesis operons, comparing sequential timepoints. Only statistically significant (adj.  $p < 0.05$ ) scores are shown. (E) Measurement of the adjusted t-statistic (12) in the RB-Tn assay on all days where fitness score was measurable (D1-3) shows that gene insertions in CPS4 consistently result in significant declines in mutant fitness for all genes within the CPS4 locus except for BT1338. See also Table S5.